Characterization of erasin (UBXD2): a new ER protein that promotes ER-associated protein degradation

Jing Liang[1,2,*,‡], Chaobo Yin[2,*], Howard Doong[2], Shengyun Fang[1,2], Corrine Peterhoff[3], Ralph A. Nixon[3] and Mervyn J. Monteiro[1,2,§]

[1]Graduate Program in Molecular Medicine, and Institute for Neurodegenerative Diseases and [2]Medical Biotechnology Center, University of Maryland Biotechnology Institute, 725 West Lombard Street, Baltimore, MD 21201, USA
[3]Center for Dementia Research, Nathan S. Kline Institute, 140 Old Orangeburg Road, Orangeburg, NY 10962, USA

*These authors contributed equally to this work
‡Present address: Department of Biochemistry and Molecular Biology, Peking University Health Science Center, 38 Xue Yuan Road, Beijing, China
§Author for correspondence (e-mail: monteiro@umbi.umd.edu)

Accepted 11 July 2006
Journal of Cell Science 119, 4011-4024 Published by The Company of Biologists 2006
doi:10.1242/jcs.03163

Summary

Ubiquitin regulator-X (UBX) is a discrete protein domain that binds p97/valosin-containing protein (VCP), a molecular chaperone involved in diverse cell processes, including endoplasmic-reticulum-associated protein degradation (ERAD). Here we characterize a human UBX-containing protein, UBXD2, that is highly conserved in mammals, which we have renamed erasin. Biochemical fractionation, immunofluorescence and electron microscopy, and protease protection experiments suggest that erasin is an integral membrane protein of the endoplasmic reticulum and nuclear envelope with both its N- and C-termini facing the cytoplasm or nucleoplasm. Localization of GFP-tagged deletion derivatives of erasin in HeLa cells revealed that a single 21-amino-acid sequence located near the C-terminus is necessary and sufficient for localization of erasin to the endoplasmic reticulum. Immunoprecipitation and GST-pulldown experiments confirmed that erasin binds p97/VCP via its UBX domain. Additional immunoprecipitation assays indicated that erasin exists in a complex with other p97/VCP-associated factors involved in ERAD. Overexpression of erasin enhanced the degradation of the ERAD substrate CD3δ, whereas siRNA-mediated reduction of erasin expression almost completely blocked ERAD. Erasin protein levels were increased by endoplasmic reticulum stress. Immunohistochemical staining of brain tissue from patients with Alzheimer's disease and control subjects revealed that erasin accumulates preferentially in neurons undergoing neurofibrillary degeneration in Alzheimer's disease. These results suggest that erasin may be involved in ERAD and in Alzheimer's disease.

Key words: Endoplasmic reticulum, UBXD2, Membrane topology, p97/VCP, ER-associated protein degradation, Alzheimer's disease

Introduction

The endoplasmic reticulum (ER) is the fundamental eukaryotic organelle where most transmembrane and secretory proteins are synthesized, and where stringent quality control systems operate to ensure that only correctly folded and properly assembled proteins are allowed to exit the site for delivery to their eventual destinations. Accordingly, misfolded and unassembled proteins (e.g. orphan receptors) are recognized and retained in the ER by the quality control apparatus, where they are extracted, polyubiquitylated, and finally degraded in the cytoplasm by the multi-subunit 26S proteasome complex, in a regulated process called ER-associated protein degradation (ERAD) (reviewed by Hampton, 2002; Tsai et al., 2002; Meusser et al., 2005).

The factors involved in ERAD are beginning to be identified (reviewed by Meusser et al., 2005). One of the key players involved in ERAD is the Cdc48 protein in yeast, or the mammalian homolog sometimes referred to as either p97 or valosin-containing protein (VCP: henceforth referred to as p97/VCP), a AAA-ATPase molecular chaperone that has been implicated in a variety of cell functions, including proteolysis, membrane fusion, and cell-cycle regulation (for reviews, see Woodman, 2003; Cao et al., 2003; Dreveny et al., 2004b; Wang et al., 2004). The diversity of p97/VCP function is believed to depend on the composition of the complex it forms with its different binding partners. For example, when bound to the heterodimeric Ufd1/Npl4 complex, p97/VCP functions in ERAD (Ye et al., 2001; Bays et al., 2001; Braun et al., 2002; Rabinovich et al., 2002; Jarosch et al., 2002), whereas when bound to p47 it functions in membrane fusion (Kondo et al., 1997; Roy et al., 2000; Hetzer et al., 2001). Interestingly, p47 and the Ufd1/Npl4 complex bind p97/VCP in a mutually exclusive manner (Meyer et al., 2000), which is perhaps not surprising, given that differential binding could provide the basis for the specificity of different p97/VCP functions.

Because p97/VCP function is dictated in part by the protein to which it binds, it is important to obtain a global understanding of its different binding factors. Towards this goal, studies have focused on proteins containing a ubiquitin regulatory X (UBX) domain (Buchberger et al., 2001; Buchberger, 2002), because it appears to be a general p97/VCP-binding module (Decottignies et al., 2004; Dreveny et al., 2004a; Schuberth et al., 2004; Hartmann-Petersen et al., 2004). The UBX domain is composed of 80 amino acids that fold with a tertiary structure very similar to that of ubiquitin (Buchberger et al., 2001; Yuan et al., 2001). The structural

basis of p97/VCP interaction with UBX domains was nicely documented using the UBX domain of the well-known p97/VCP interactor, p47 (Yuan et al., 2001; Dreveny et al., 2004a; Dreveny et al., 2004b). It was found that a loop region in the p47 UBX domain, which is conserved in many other UBX domains, but missing in ubiquitin, binds a hydrophobic pocket in p97/VCP, although other binding sites are also thought to exist (Uchiyama et al., 2002).

A systematic analysis of the seven UBX domain-containing proteins in yeast confirmed that all of them bind Cdc48, as expected (Decottignies et al., 2004; Hartmann-Petersen et al., 2004; Schuberth et al., 2004). Interestingly, some of these UBX proteins were found to be membrane associated, possibly to the ER (Decottignies et al., 2004; Schuberth and Buchberger, 2005; Neuber et al., 2005). Recently two different groups described the properties of one such protein called Ubx2 (Schuberth and Buchberger, 2005; Neuber et al., 2005). They both found that Ubx2 binds Cdc48 and that deletion of Ubx2 retards ERAD, suggesting that Ubx2 is a positive-regulator of ERAD.

In order to characterize the function of other UBX-containing proteins, particularly those in mammals, which apart from p47 have remained poorly characterized, we focused on human UBXD2, an annotated but uncharacterized UBX-containing protein. Using a combination of cell biological, immunological and biochemical approaches, we demonstrate that UBXD2 is an integral ER and nuclear-envelope-associated protein that is expressed in all mammalian cells and tissues examined, and which is conserved across species. We show that the UBX domain of UBXD2 is indeed involved in binding p97/VCP. Furthermore, we demonstrate that overexpression of UBXD2 enhances the degradation of a classical ERAD substrate whereas a siRNA-mediated reduction in UBXD2 expression levels almost completely blocked ERAD. We further demonstrate that UBXD2 levels are increased in cells treated with agents that induce ER stress and that anti-UBXD2 staining is increased in neuropathological lesions in brains of patients with Alzheimer's disease (AD). Because of these new insights we have chosen to refer to this novel human protein as erasin, to signify a protein involved in clearing ERAD substrates (an ERAD substrate erasing protein).

Results

Human erasin is a ubiquitously expressed protein that is conserved across species

The human *UBXD2* gene is located on chromosome 2q21.3-q22.1 according to the completed human genome sequence (gene ID 23190, locus tag HGNL:14860). To obtain a cDNA encoding UBXD2 we sequenced several human EST cDNA clones and identified one that contained the complete *UBXD2* open reading frame (ORF). Based on its properties, described below, we propose to rename the protein erasin.

The inferred ORF of human erasin predicts a protein of 508 amino acids (Fig. 1A), and contains the following key structural motifs: a putative coiled-coil domain (residues 192-282), a UBX domain (residues 316-395) (Buchberger et al., 2001), and a conspicuous hydrophobic domain (residues 414-434). Through database searches we identified erasin homologs in most eukaryotes, some of which are shown in Fig. 1A. Among them, mouse erasin protein is 93% identical to its human counterpart, indicating that erasin is highly conserved in mammals. Comparison of the human erasin protein with all seven UBX-containing proteins of yeast indicated weak sequence homology with all of them, the highest being with Ubx7, which shares 20.6% identity, and 32% similarity. This suggests that erasin protein may have evolved for some specialized function in mammals, which might not be present in yeast. To obtain possible clues as to the function of mammalian erasin we examined the information that has been published on the yeast Ubx7 protein (also called Cui3p), to see if the two are indeed related, but found it to be uninformative because yeast strains deleted of the Ubx7 gene are viable and have no noticeable phenotype, apart from a slight defect in sporulation (Decottignies et al., 2004). A reconstructed phylogenetic tree (Fig. 1B) generated using the AssemblyLIGN program suggests that the erasin genes might have evolved from single-cell eukaryotic organisms to mammals.

We next studied the RNA and protein expression pattern of erasin in mammals. Northern blot analysis revealed that *ERASIN* mRNA is expressed at variable levels as a single major 3.9 kb transcript in all adult human tissues examined (Fig. 2B). To study erasin protein expression we generated two rabbit polyclonal anti-erasin antibodies, 130 and 141, to the N- and C-terminal regions of human erasin, respectively (Fig. 2A,C). Both antibodies recognized a major 64 kDa band, as well as few minor smaller and larger bands, in immunoblots of HeLa cell lysates (Fig. 2C). They are highly specific for erasin because their preimmune sera did not recognize similar size protein bands (data not shown) and because the immunoreactive bands recognized by antibody 141 could be competed away with increasing amounts of its cognate peptide (Fig. 2D). The 64 kDa band that was recognized by the two antibodies probably corresponds to the full-length (FL) erasin polypeptide for the following reasons. First, the predicted mass of the protein is approximately the same size. Second, overexpression of the complete erasin ORF increased immunoreactivity of the 64 kDa band (Fig. 2E). Third, Myc- and GFP-tagged erasin constructs produced the expected shift in the size of the protein (Fig. 2E and Fig. 4C). Fourth, in vitro transcription and translation of FL erasin cDNA yielded a radiolabeled band of 64 kDa (see Fig. 6C).

Immunoblot analysis indicated that erasin is expressed in all human cell lines tested, with the highest expression detected in HEK293 cells after normalization for actin loading (Fig. 2F). In addition, immunoblot analysis of equal amounts of protein lysate prepared from adult mouse tissues indicated that erasin is ubiquitously expressed, with the highest expression seen in the brain (Fig. 2G upper panel). It should be noted that the mouse tissue blot, when reblotted for actin, revealed differences in the levels of the protein in the different tissue samples (Fig. 2G bottom panel), probably owing to a variation in the amount of actin that is present in different tissues. It is interesting to note that *ERASIN* mRNA is expressed at relatively low levels in human brain, whereas erasin protein is expressed at high levels in mouse brain. This difference could stem from translation regulation of erasin, or from differences inherent in comparing human and mouse tissues.

Erasin localizes to the ER

We used immunofluorescence light microscopy and subcellular fractionation to determine the site of erasin localization in

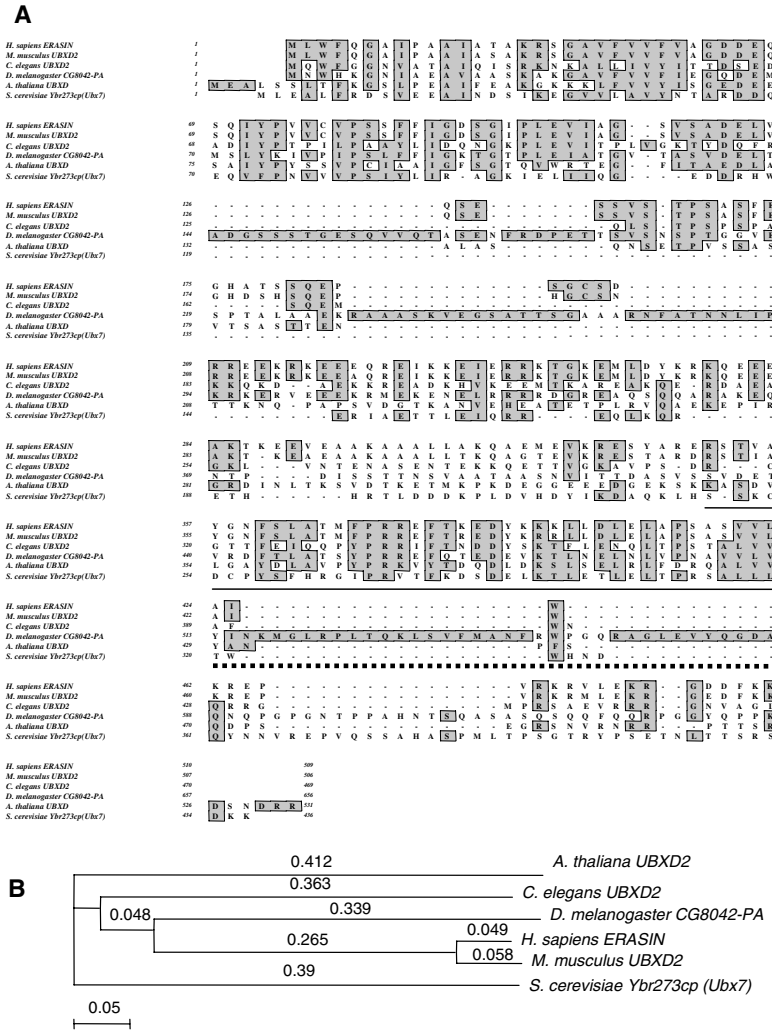

Fig. 1. Homology of erasin proteins found in different species. (A) Sequence alignment of erasin proteins in selective eukaryotic organisms. Homologous amino acids in four or more sequences, including gaps, are shaded. The UBX domain is underlined. The dashed line is the sequence that covers the region that was necessary and sufficient for ER targeting. (B) Reconstructed phylogenetic tree of the erasin homologs using the AssemblyLIGN software.

cells. Both anti-erasin antibodies revealed reticular staining of the cytoplasm of untransfected HeLa and HEK293 cells, a pattern that was not displayed by their preimmune serum (Fig. 3Aa,b; data for serum 141 not shown). The staining was stronger upon overexpression of untagged FL erasin cDNA (Fig. 3Ac). An essentially identical pattern was observed upon live imaging of cells expressing a GFP-tagged FL erasin construct (see Fig. 5Ba). Double-immunofluorescence microscopy revealed excellent colocalization of the erasin staining pattern with calnexin, a protein marker of the ER (Fig. 3Ad-f). Furthermore, we found that endogenous FL erasin polypeptide was present in predominantly the same fractions of cell homogenates separated on iodixanol gradients as calnexin, with a very minor fraction of the protein overlapping the Golgi marker golgin-97 (Fig. 3B). Interestingly, a major proteolytically cleaved form of erasin that is recognized by the N-terminal- but not the C-terminal-specific erasin antibody (Fig. 3B and data not shown), separated in lighter fractions of the gradients, suggesting that this cleaved form of erasin maybe localized to a distinct subcellular compartment compared with the FL protein. Together, these results strongly indicate that FL erasin is predominantly located in the ER.

Erasin is an ER membrane-associated protein whose N- and C-termini face the cytoplasm

To determine whether erasin resides within the lumen or is embedded in the membrane of the ER, we used HEK293 cells to prepare reticuloplasm (the luminal material of the ER) as well as the nuclear, membrane, and soluble cytosolic fractions and used them for immunoblot analysis of erasin. As shown in Fig. 3C, endogenous erasin was present solely in the membrane fraction. By contrast, two known ER luminal proteins, BiP and calreticulin, were found in the reticuloplasm fraction as expected, but also in the membrane and soluble fractions, probably because of incomplete lysis and premature disruption of the ER contents, respectively.

Neither high salt (1 M NaCl) nor high pH (pH 11) conditions was capable of extracting erasin from a HEK293 membrane

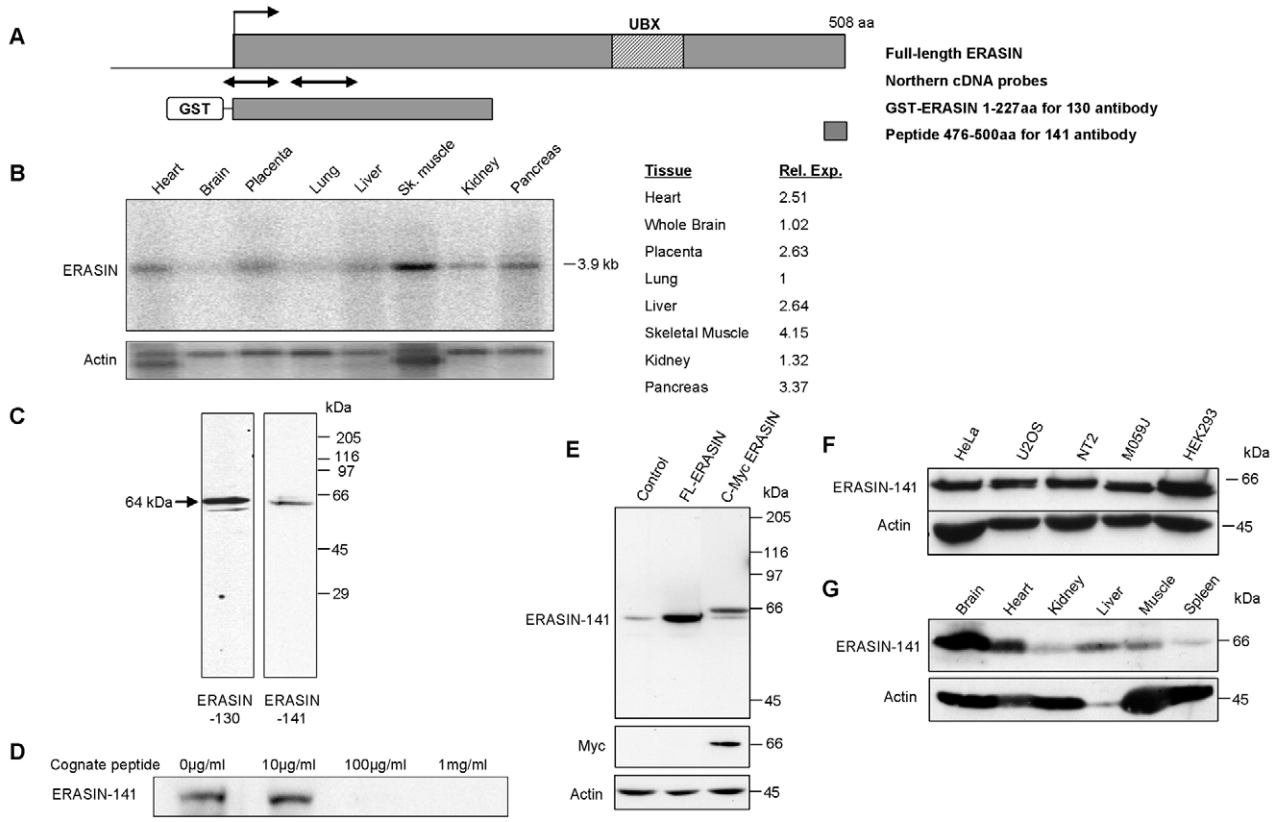

Fig. 2. Erasin is widely expressed in different tissues. (A) A schematic drawing of the erasin protein. The inferred erasin ORF consists of 508 amino acids. The protein contains a UBX domain from residues 316 to 395 (striped). The probes used in northern blot assay are indicated. Also shown are the two regions against which rabbit polyclonal anti-erasin antibodies 130 and 141 were raised. (B) Northern blot of *ERASIN* mRNA expression in multiple human tissues. After stripping, the blot was reprobed with β-actin. The level of *ERASIN* mRNA expression relative to that in the lung is shown after normalization for actin loading. (C) Characterization of anti-erasin antibodies. Endogenous erasin protein in HeLa cell lysates detected with anti-erasin antibodies 130 and 141. Both antibodies detected a major 64 kDa band that was not detected by their respective preimmune sera (for the preimmune 141 serum see Fig. 6A lane 1). (D) Peptide competition assay demonstrating specificity of antibody 141. Same procedure as Fig. 2C, except antibody 141 was pre-incubated with 0-1 mg/ml of its cognate peptide for 2 hours before immunoblotting. (E) Protein lysates of HeLa cells mock transfected (Control), or transfected with FL untagged erasin, or a C-Myc-tagged erasin expression constructs immunoblotted with anti-erasin 141 (top panel), anti-Myc (middle panel) and anti-actin (bottom panel) antibodies. (F) Immunoblots showing endogenous erasin protein levels in different human cell lines revealed by anti-erasin antibody. (G) Equal amounts of protein lysates from different mouse tissues immunoblotted for erasin with antibody 141 (upper panel) and subsequently with an anti-actin antibody (lower panel).

fraction (Fig. 3D), suggesting that erasin is an integral, rather than a peripheral ER membrane protein. As expected, erasin was solubilized after disruption of membranes using the detergent Triton X-100. The same properties were displayed by calnexin, a known integral ER membrane protein. By contrast, GM130, a known peripheral Golgi protein, was extracted by high pH but not by high salt conditions. The unusual retention of GM130 in the pellet fraction after Triton X-100 is consistent with an earlier report (Nakamura et al., 1995).

We used protease protection assays to examine the membrane topology of erasin (Fig. 4). For these assays, microsomes isolated from HeLa cells were incubated with increasing amounts of proteinase K, and the digestion products analyzed for immunoreactivity with antibodies specific for the N- and C-terminal regions of erasin. We monitored the digestion using endogenous calnexin as a control. Calnexin is a known ER transmembrane protein oriented with its N-terminus in the lumen and C-terminus in the cytosol (Wada et al., 1991) (see Fig. 4A). In accord with this topology, immunoreactivity of the C-terminus of calnexin was lost upon digestion with increasing amounts of proteinase K (Fig. 4A). By contrast, immunoreactivity of the N-terminal portion of calnexin persisted in the same lysates, and moreover, the 88 kDa intact polypeptide was digested to a smaller 66 kDa protected fragment (reflecting digestion of the C-terminal tail). By comparison, parallel immunoblots of the same lysates with anti-erasin antibodies revealed a proteinase K dose-dependent loss of immunoreactivity with both the N- and C-terminal erasin antibodies (Fig. 4B). Because our model of the topology of erasin suggested that it has a short C-terminus that protrudes from membranes (see below), it remained possible that such a small, protected fragment might not be detected on our immunoblots. We therefore repeated the proteinase K digestion assay using a C-terminus GFP-tagged erasin construct, but failed to observe any protection of the longer GFP-fused C-terminal fragment (Fig. 4C).

Results of these protease protection assays suggested that

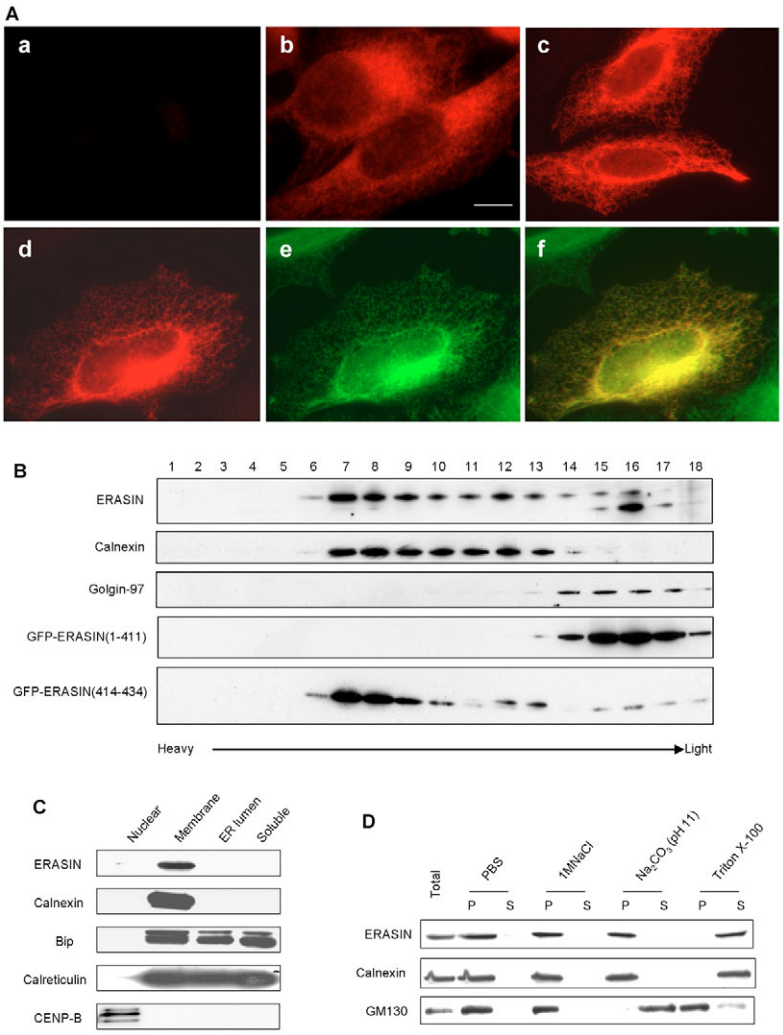

Fig. 3. Erasin localizes to the ER.
(A) Immunofluorescence microscopy. (a-c) Indirect immunofluorescence microscopy of HeLa cells probed with the preimmune 130 serum (a) or with the anti-erasin 130-immune serum (b and c). Cells in panels a and b were untransfected whereas those in panel c were transfected with a FL untagged erasin cDNA expression plasmid. (d-f) Colocalization of erasin and calnexin. HeLa cells transfected with C-Myc erasin and revealed with monoclonal anti-Myc antibody (d), endogenous calnexin revealed with rabbit polyclonal anti-calnexin antibody (e), and the result of merging the erasin and calnexin images (f). Bar, 5 μm for all panels.
(B) Immunoblots showing distribution of proteins in HeLa cell homogenates fractionated on 0-25% iodixanol gradients. The upper three panels show the distribution of endogenous erasin, calnexin, and golgin-97 proteins. The lower two panels show the distribution of the two different GFP-tagged erasin constructs expressed in HeLa cells. (C) Immunoblots showing erasin is only found associated with a membrane fraction and is not present in soluble, ER-luminal or nuclear fractions. The different fractions were prepared as described in the Materials and Methods. Controls showing fractionation of calnexin, an ER-membrane associated protein, BiP and calreticulin, two ER luminal proteins, and CENP-B, a nuclear protein. (D) HeLa cell lysates were separated into pellet (P) and supernatant (S) fractions in 1× PBS, in 1 M NaCl, in 0.1 M Na_2CO_3 (pH 11) or in 1% Triton X-100. These fractions were analyzed by immunoblotting using anti-erasin, anti-calnexin and anti-GM130 antibodies. GM130 is a known peripheral Golgi protein used here as a control.

both the N- and C-termini of erasin face the cytoplasm. We confirmed this orientation by immunoelectron microscopy of HeLa cells overexpressing FL untagged erasin. As shown in Fig. 4D-F, both N- and C-terminal-specific erasin antibodies predominantly decorated nuclear envelope (NE) and ER membranes with gold particles on the cytoplasmic and nucleoplasmic sides, but rarely within the lumen of the membranes. These results further indicate that erasin is localized to the NE, which is contiguous with the ER (Franke et al., 1981).

The erasin sequence from 414 to 434 is both necessary and sufficient for ER targeting

To identify the ER-targeting sequences we fused GFP in-frame at different points of the erasin ORF (Fig. 5A) and determined which, if any, of the fusion proteins localized to the ER by live cell imaging and fractionation studies of transfected HeLa cells. An examination of a series of progressive C-terminal deletions of the erasin ORF revealed that ER targeting is lost upon truncation of the erasin polypeptide to a length of 411 aa and smaller (see Fig. 3B fifth panel and Fig. 5Bd). Moreover, a C-terminal erasin fragment spanning residues 414 to the C-terminus was targeted to the ER, suggesting that the targeting sequence is contained within this region (data not shown). Because the hydrophobicity profile of erasin indicated the presence of a highly hydrophobic sequence (residues 414-434) within the C-terminal targeting sequence, we constructed an additional construct by fusing GFP to the hydrophobic patch (HP) and found that the HP was sufficient for ER targeting (Fig. 3B bottom panel and Fig. 5Bf). Furthermore, an erasin-GFP fusion construct deleted of the HP was not targeted to the ER (data not shown). On the basis of these GFP targeting results and the results of the immunogold localization and protease protection assays, we propose that the HP of erasin (i.e. sequence 414-434) anchors the protein to the ER membrane, as depicted by the model shown in Fig. 4B. Interestingly, the HP resembles the membrane-targeting sequence of caveolin-1 (Fig. 5C; see Discussion for further details).

Erasin binds p97/VCP

Erasin contains a UBX domain, which appears to be a general domain involved in binding p97/VCP (reviewed by Dreveny et al., 2004b; Schuberth et al., 2004). To determine whether erasin forms a complex with p97/VCP in cells, we immunoprecipitated erasin from HeLa lysates using the anti-erasin antibody 141 and examined the precipitates for the presence of p97/VCP by immunoblotting (Fig. 6A). The

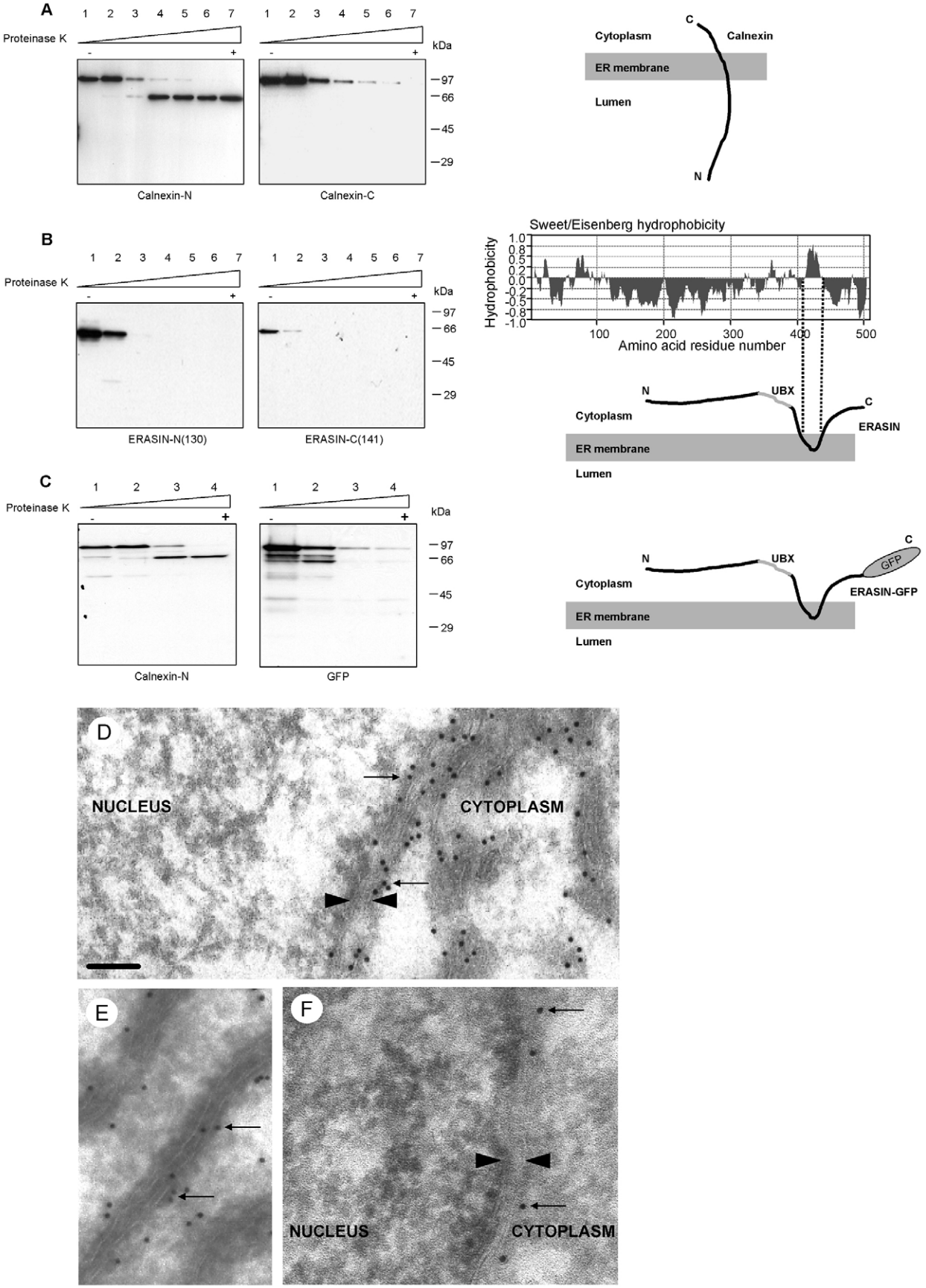

Fig. 4. See next page for legend.

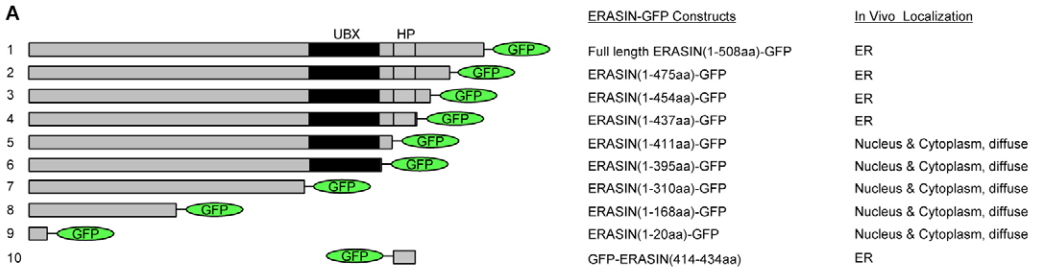

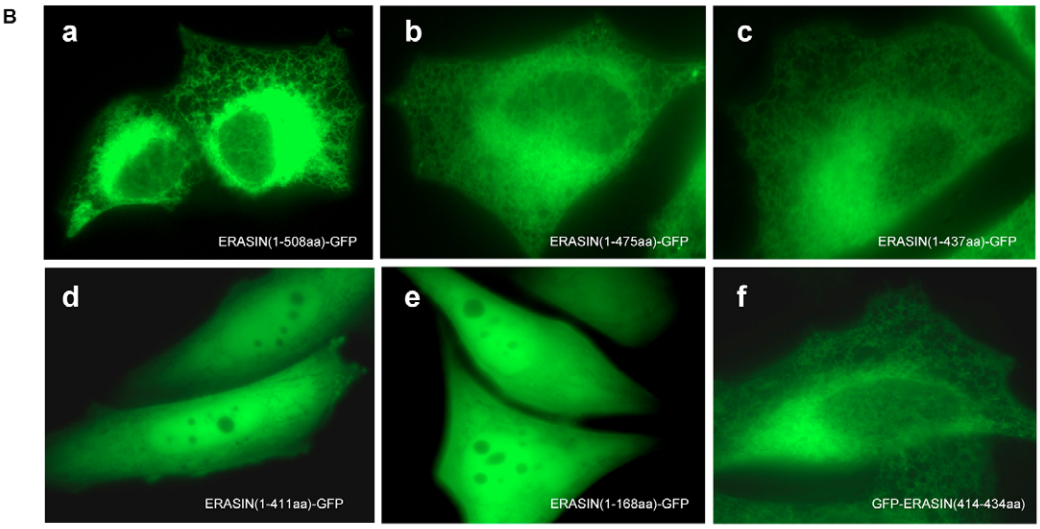

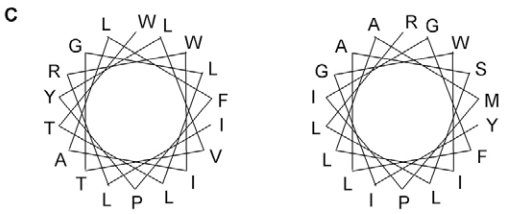

Fig. 5. GFP-tagging experiments indicate that the erasin sequence between residues 414 to 434 is both necessary and sufficient for ER localization. (A) Schematic diagram of GFP-tagged erasin constructs and summary of their localization obtained by live cell imaging and biochemical fractionation on gradients. The hydrophobic patch (HP) that is responsible for ER localization is indicated. (B) Representative examples of the fluorescent images taken of live cells following transfection with different GFP-tagged erasin constructs. (C) Helical wheel representation of the hydrophobic targeting sequence and comparison with that of caveolin-1. Note the position of the putative helix-disrupting proline residue in both sequences (see text).

Fig. 4. Proteinase K protection assay used to reveal the membrane topology of erasin. Microsome membranes were prepared from HeLa cells and incubated with increasing amounts of proteinase K (0 μg/ml for lane1, 0.25 μg/ml for lane2, 1 μg/ml for lane 3, 10 μg/ml for lane 4, 100 μg/ml for lane 5, these samples were treated with proteinase K for 5 minutes; and 10 μg/ml for lane 6 and lane 7, 10 μg/ml and 100 μg/ml proteinase K were incubated with the samples for 1 hour). (A) Immunoblots of the proteinase-K-treated lysates probed with either anti-calnexin-N, and anti-calnexin-C antibodies or (B) anti-erasin 130 and 141 antibodies. (C) Repeat of a similar experiment using a C-terminus GFP-tagged erasin construct and probed with anti-calnexin-N or anti-GFP antibodies. Schematic drawings on the right side depict the known membrane topology of calnexin and of erasin as we propose here. Our model suggests that erasin is anchored in the ER or NE by a hydrophobic patch located between residues 414-434 (see hydrophobicity profile in B) and that both its N- and C-terminus including its hydrophobic domain face the cytoplasm or nucleoplasm. (D,E) Immunogold microscopy of HeLa cells transfected with FL erasin cDNA and probed with anti-N-terminal (130) (D and E) and anti-C-terminal (141) (F) specific erasin antibodies. The majority of gold particles (D,E, arrows) are located on both the nucleoplasmic and cytoplasmic sides of the NE and ER, respectively, with very few particles, if any, in the lumen (the position of the double membrane is indicted by the arrowheads). Immunoreactivity with the C-terminal antibody was weaker, but it too decorated gold particles on the cytoplasmic side of the NE (arrows in F). Bar, 5 nm.

preimmune 141 serum was used as a control to demonstrate the specificity of the immunoprecipitation. As expected, the immune 141 serum precipitated erasin and pre-immune serum did not (Fig. 6A top panel, lanes 2 and 1, respectively). Interestingly, p97/VCP was co-precipitated with erasin in untransfected HeLa cell lysates (second panel lane 2), and, as expected, was not co-precipitated with the preimmune serum (second panel, lane 1). The specificity of the immunoprecipitation can be seen by the absence of calnexin in these immunoprecipitates (third panel), which, like erasin is localized to the ER (see below). Interestingly, more endogenous p97/VCP was immunoprecipitated in cells in which erasin was overexpressed (Fig. 6A second panel, lane 3), consistent with the notion that erasin can bind p97/VCP. To confirm that erasin and p97/VCP bind directly to one another, we conducted GST pull-down assays, incubating purified recombinant bacterially His-tagged p97/VCP with either FL erasin GST-fusion protein or GST alone. p97/VCP was pulled down by GST-erasin fusion protein but not by GST alone (Fig. 6B), indicating that erasin and p97/VCP bind directly to one another. To locate the p97/VCP-binding region in erasin we performed additional GST pull-down assays, examining the binding of purified GST-p97/VCP fusion protein with different portions of radiolabeled erasin polypeptides. These in vitro assays revealed that the UBX domain of erasin is critical for p97/VCP binding because erasin polypeptides containing the domain were efficiently pulled down by the GST-p97/VCP fusion protein whereas those lacking the domain displayed weak binding (Fig. 6C). We confirmed that the UBX domain of erasin is indeed required for forming a complex with p97/VCP in cells using co-immunoprecipitation assays. In these assays we found more p97/VCP was co-

immunoprecipitated with erasin protein in cells transfected with a Myc-tagged FL erasin expression construct compared to cells transfected with a similar construct, but deleted of the UBX domain (Fig. 6D).

Reduction of erasin levels by RNA interference leads to inhibition of ERAD

The possible functional significance of the interaction of erasin with p97/VCP was further explored. To this end, we examined whether erasin is involved in ERAD because the erasin protein has a similar topology to that of UBX2, the recently described yeast UBX-containing protein that was found to positively regulate ERAD (Schuberth and Buchberger, 2005; Neuber et al., 2005). To explore this possibility we examined whether modulation of erasin protein levels in cells affects the rate of protein turnover of the classical ERAD substrate CD3δ (Klausner et al., 1990), whose degradation is p97/VCP dependent (Zhong et al., 2004).

In preliminary studies we found that transfection of HEK293 cells with 5-20 nM concentration of siRNAs, designed to specifically induce genetic interference of erasin, was effective at reducing erasin protein levels by ~80% (data not shown). As expected, transfection of HEK293 cells with a control siRNA, designed not to induce interference of any known gene, did not alter erasin protein levels (data not shown). Having established the procedures to successfully manipulate erasin protein levels (i.e. reduce its levels by RNA interference and increase its levels by the overexpression of *ERASIN* cDNA) we compared the rate of CD3δ protein turnover over a 7.5 hour period in HEK293 cells treated with cycloheximide (to inhibit new protein synthesis) in which erasin levels were not intentionally manipulated with those in which erasin levels were either increased or decreased. By these studies we found that erasin protein knockdown dramatically reduced CD3δ protein turnover compared with cells in which erasin levels were not manipulated, whereas overexpression of erasin slightly increased CD3δ protein turnover (Fig. 7A,B).

To investigate whether an alteration in erasin protein levels affects the degradation of a soluble protein we measured the turnover of GFP^{u}, a short-lived protein (Bence et al., 2001), using classical pulse-chase studies. As shown in Fig. 7C,D, unlike CD3δ, the turnover of GFP^{u} was not substantially altered in cells in which erasin levels were either increased or decreased, compared with cells in which erasin levels were not intentionally manipulated.

Because our results suggested that erasin is involved in ERAD we examined whether erasin forms a complex with other ERAD components. Using immunoprecipitation assays

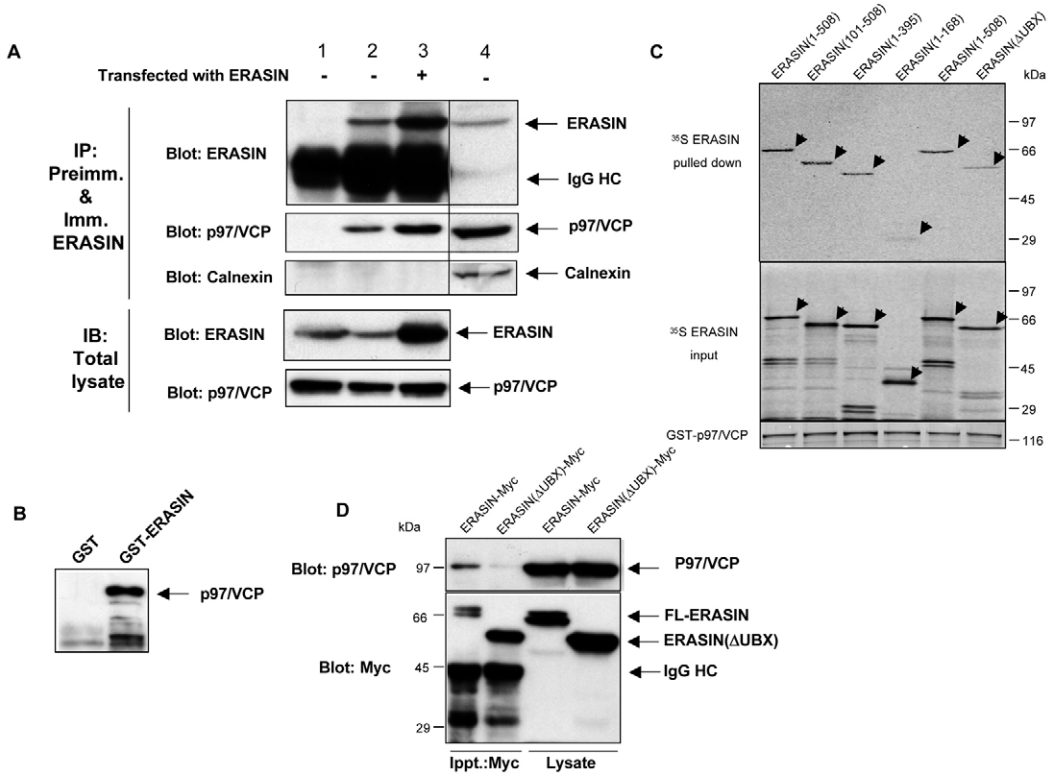

Fig. 6. Erasin binds p97/VCP proteins primarily through its UBX domain. (A) Immunoprecipitation assays demonstrating that erasin forms a complex with p97/VCP. Lysates were prepared from HeLa cells that were either left untransfected (lanes 1 and 2), or transfected with a FL untagged erasin cDNA plasmid (lane 3), and used to immunoprecipitate erasin using the preimmune 141 serum (lane 1) or with anti-erasin antibody 141 (lanes 2 and 3). Lane 4 contains 1/10 of the lysate prepared from untransfected cells that was used for the immunoprecipitation shown in lane 1 and 2. After separation by SDS-PAGE, the immunoprecipitates were immunoblotted for erasin, p97/VCP and calnexin proteins (upper three panels, respectively). The bottom two panels show 1/10 the amount of total protein lysates from the same sets of cells immunoblotted for erasin, and p97/VCP. (B) Immunoblot demonstrating recombinant p97/VCP is pulled down by GST-erasin fusion protein but not by GST alone. (C) GST pull-down assays showing that erasin binds p97/VCP primarily through its UBX domain. In vitro translated ^{35}S-radiolabeled proteins generated from different erasin constructs (labeled; arrows indicate the major erasin translation product) were analyzed for binding FL p97/VCP GST-fusion protein by pull-down assays (upper panel, autoradiogram of the pull-down results; middle panel, 1/10 portion of the input sample; lower panel, Coomassie-stained gel of pulled down GST-p97/VCP-fusion protein). (D) Immunoprecipitation assays demonstrating that the UBX domain of erasin is important forming a complex with p97/VCP in cells. Lysates prepared from HeLa cells transfected with either FL Myc-tagged erasin or Myc-tagged erasin with deleted UBX domain (ΔUBX) were used to conduct immunoprecipitations with a mouse anti-Myc antibody. The immunoprecipitates, together with 1/10 portion of the lysate, were immunoblotted with anti-p97/VCP (upper panel) and anti-Myc antibodies (lower panel).

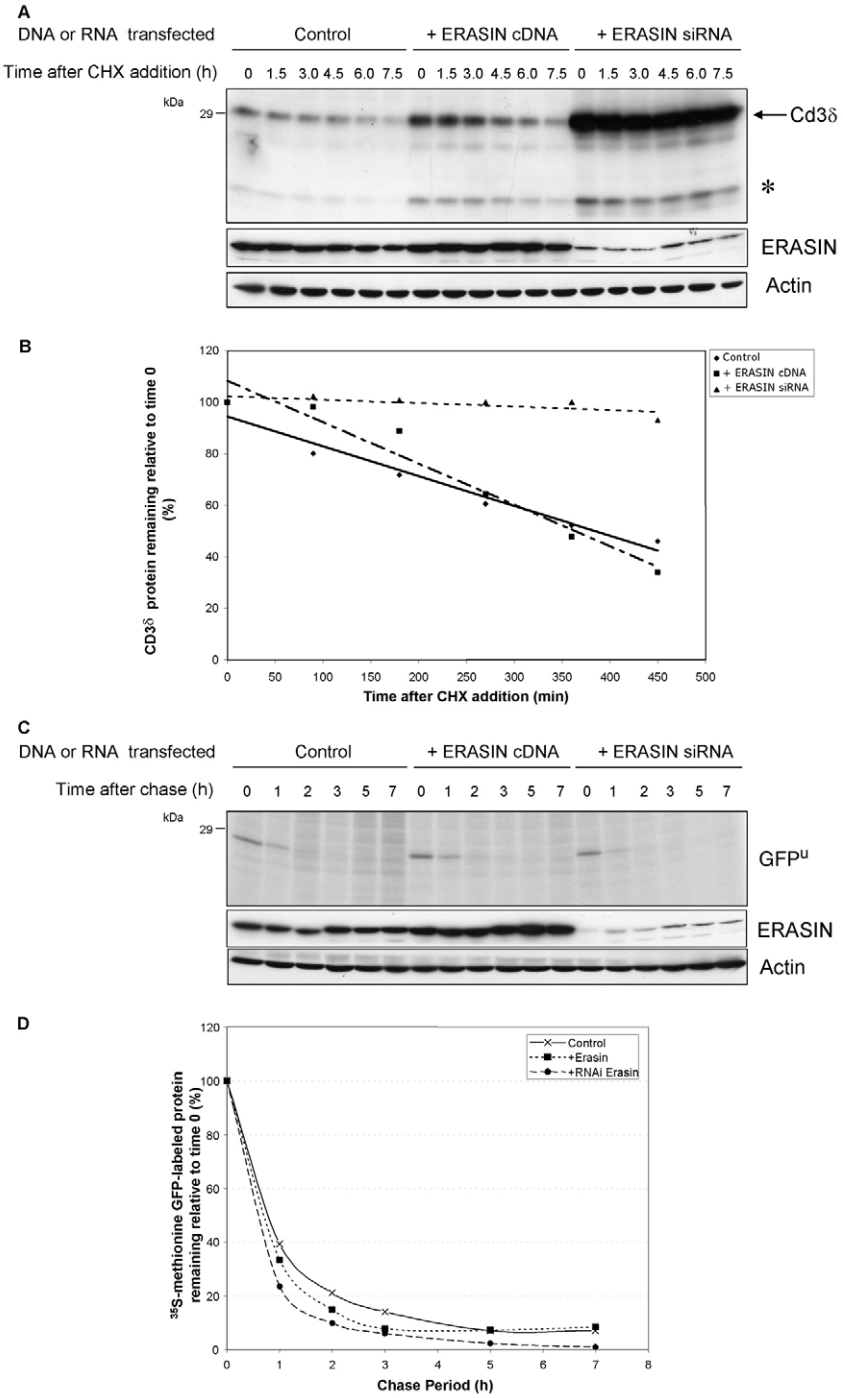

Fig. 7. A reduction of erasin levels inhibits ERAD. (A) HEK293 cell cultures were cotransfected with constant amounts of HA-CD3δ, together with either *ERASIN* cDNA expression plasmid, or empty vector plasmid, or with 10 nm SMARTpool *ERASIN* siRNAs. For the knockdown experiments, the cells were transfected with the siRNAs 20 hours before transfection with CD3δ. 20 hours after CD3δ transfection, cycloheximide was added to all cultures and protein lysates were collected at the time intervals indicated. Equal amounts of protein lysates were then immunoblotted for erasin, HA and actin. The arrow and the asterisk indicate the glycosylated and non-glycosylated forms of CD3δ, respectively. (B) Densitometric analysis of the bands shown in A and expressed relative to the level present at the 0 time point. The Microsoft Excel program was used to produce a best-fit line for each experimental set. (C) A HEK293 cell line stably expressing GFP^u was transfected with the nucleic acids as described in A, but omitting HA-CD3δ. The turnover of GFP^u in the different transfected cells was determined by classical pulse-chase studies of [^{35}S]methionine-labeled and immunoprecipitated GFP proteins over a 7-hour period (upper panel). Immunoblot analysis of the cell lysates used for the immunoprecipitation studies confirmed that erasin levels were altered in the expected manner (middle panel), with actin loading of these lysates confirming equal protein loading of the lysates (bottom panel). (D) Graph showing the exponential decline of pulse-labeled GFP^u protein over time. The turnover of GFP^u was altered little in the three experimental sets.

(Fig. 8A,B) we found that erasin was present in complexes containing the autocrine motility factor receptor (also called gp78), an ER-associated E3 ligase, and with the putative ER-channel forming protein Derlin-1, both of which have been shown to be important for ERAD in mammalian cells (Zhong et al., 2004; Lilley and Ploegh, 2004; Ye et al., 2004; Ye et al., 2005; Oda et al., 2006; Li et al., 2006). We next examined if the levels of various ERAD components are altered upon knockdown of erasin levels in cells. Immunoblot analysis of equal amounts of protein lysate revealed little, if any, difference in the levels of p97(VCP), gp78 and Derlin-1 proteins in cells in which erasin was knocked down compared with control cells (Fig. 8C). These results suggest that the inhibition of CD3δ degradation that we observed after knockdown of erasin levels is more likely to be a direct consequence of a reduction in erasin levels rather than due to secondary effects of an alteration in other ERAD components.

Taken together, these results strongly suggest that erasin functions by promoting ERAD and that reduction of erasin levels results in dramatic inhibition of ERAD.

Erasin is induced by ER stress

Because many proteins in the ER are induced by ER stress we examined whether erasin responds similarly. HeLa cells were treated for 17 hours with four known ER-stress-inducing reagents, tunicamycin, thapsigargin, DTT and the calcium ionophore A23187, and erasin protein levels were measured by immunoblotting (Fig. 9A). All four agents induced an increase in ERUX protein levels, which varied from two- to fourfold (Fig. 9B). The induction is noticeable but moderated compared with the strong induction of BiP, an ER-resident molecular chaperone, in the same lysates (Fig. 9A).

Pathological accumulation of erasin immunoreactivity in neurons in Alzheimer's disease

Because ER stress has been implicated in AD pathology

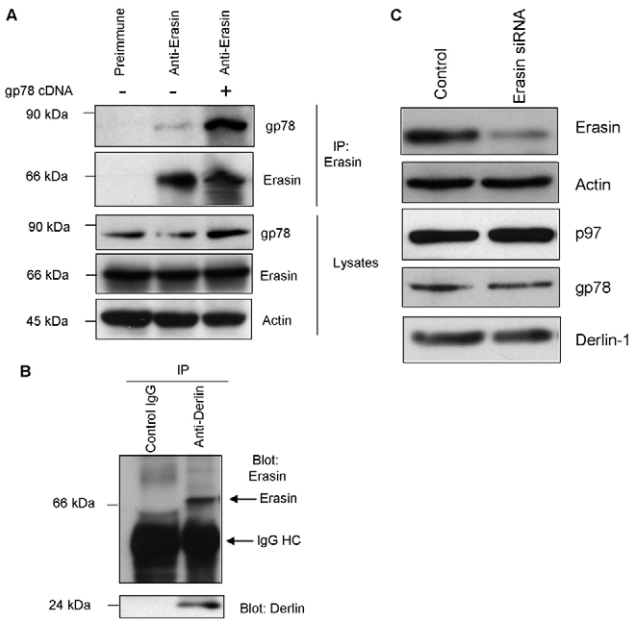

Fig. 8. Erasin is found in a complex with other ERAD components. (A) Lysates from HeLa cells transfected with a gp78-expression construct or which were left untransfected were used to conduct immunoprecipitations with anti-erasin 130 antibody or its preimmune serum. The immunoprecipitates were immunoblotted with anti-gp78 (upper panel) and anti-erasin antibodies (second panel). The levels of expression of gp78, erasin and actin in equal amounts of protein lysate from these cultures are shown in the bottom three panels. (B) Immunoprecipitation of proteins from untransfected HeLa cells using anti-Derlin-1 antibody or a control IgG antibody and immunoblotted for erasin (upper panel) or Derlin-1. (C) Immunoblot analyses of equal amounts of proteins from normal HEK293 cells (control) and in cells in which erasin levels were reduced using siRNA, probed for the different proteins as listed.

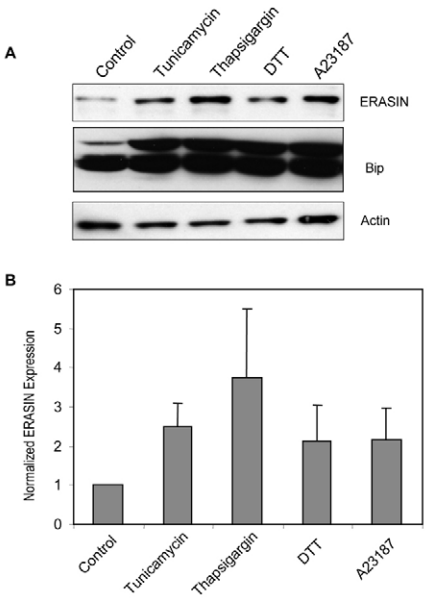

Fig. 9. Erasin is an ER stress-inducible protein. (A) HeLa cells were treated with 7 μM A23187, 2 mM DTT, 5 μM thapsigargin and 2 μg/ml tunicamycin for 16 hours. Cell lysates were collected and immunoblotted using polyclonal anti-erasin antibody 141, anti-BiP and anti-actin antibodies. (B) Levels of erasin protein (mean ± s.d.) seen after the different treatments relative to that of the untreated control were quantified from three independent experiments.

(Hoozemans et al., 2005), we investigated the possibility that erasin may also be associated with AD pathology. Using erasin 141 antiserum, we determined the distribution of erasin immunoreactivity in paraffin sections of prefrontal cortex from neuropathologically normal cases (n=7) and individuals with moderate to severe AD pathology (Braak stage VI) (n=7). In all control brains, immunoreactivity was barely discernable above background staining in occasional neurons (Fig. 10B,C) and was absent elsewhere (Fig. 10A). By contrast, strong immunoreactivity was detected in six of the seven AD brains in about 15-20% of neurons in pyramidal cell layers III and V (Fig. 10D), which was approximately the frequency of neurons exhibiting neurofibrillary pathology by Bielchowsky staining. Immunoreactivity was concentrated non-uniformly within the cytoplasm in a variable pattern that was vesicular, membranous or amorphous (Fig. 10E-I). In addition to this perikaryal labeling pattern, erasin immunoreactivity was strong in dystrophic neurites scattered through the neuropil or clustered within neuritic plaques (Fig. 10J). In immunolabeled sections counterstained with thioflavin-S, strongly immunoreactive neurons were often, though not exclusively, thioflavin-S-positive. In thioflavin-S-positive cells, immunoreactivity only partially overlapped with flame-shaped thioflavin-S-positive structures that correspond to neurofibrillary tangles (Fig. 10L,M). These results indicate that erasin accumulates in AD-afflicted brains.

Discussion

Here we described erasin, to our knowledge, the first mammalian UBX-containing protein that has been localized to the ER or NE. Several lines of evidence led us to conclude that erasin is an important protein. First, erasin is expressed in all cells and tissues we examined. Second, erasin localizes in the ER with a topology consistent with its ability to bind the AAA-ATPase molecular chaperone, p97/VCP. Third, knock down of erasin levels leads to inhibition of ERAD. Fourth, erasin levels are induced by ER stress. Finally, erasin accumulates in pathological lesions in AD-afflicted brains.

Our results from immunofluorescence staining, immunogold localization, subcellular fractionation, protease protection assays and localization of GFP-fusion deletion derivatives of erasin strongly indicate that erasin is an integral membrane protein that is targeted to ER or NE membranes through a hydrophobic sequence located close to its C-terminus. On the basis of these results we propose a model for the topology of human erasin (Fig. 4B), depicting the polypeptide ‘pinned’ to membranes by the hydrophobic patch located between residues 414-434 of the 508-amino-acid-long protein, with the remainder of the protein exposed to the cytoplasm or nucleoplasm. A question that emerges from this model concerns how the hydrophobic targeting sequence anchors erasin to the ER or NE membrane: is the sequence inserted directly into membranes or is targeting indirect, perhaps through an accessory factor? Although we do not know the answer to this question we are particularly intrigued by the fact

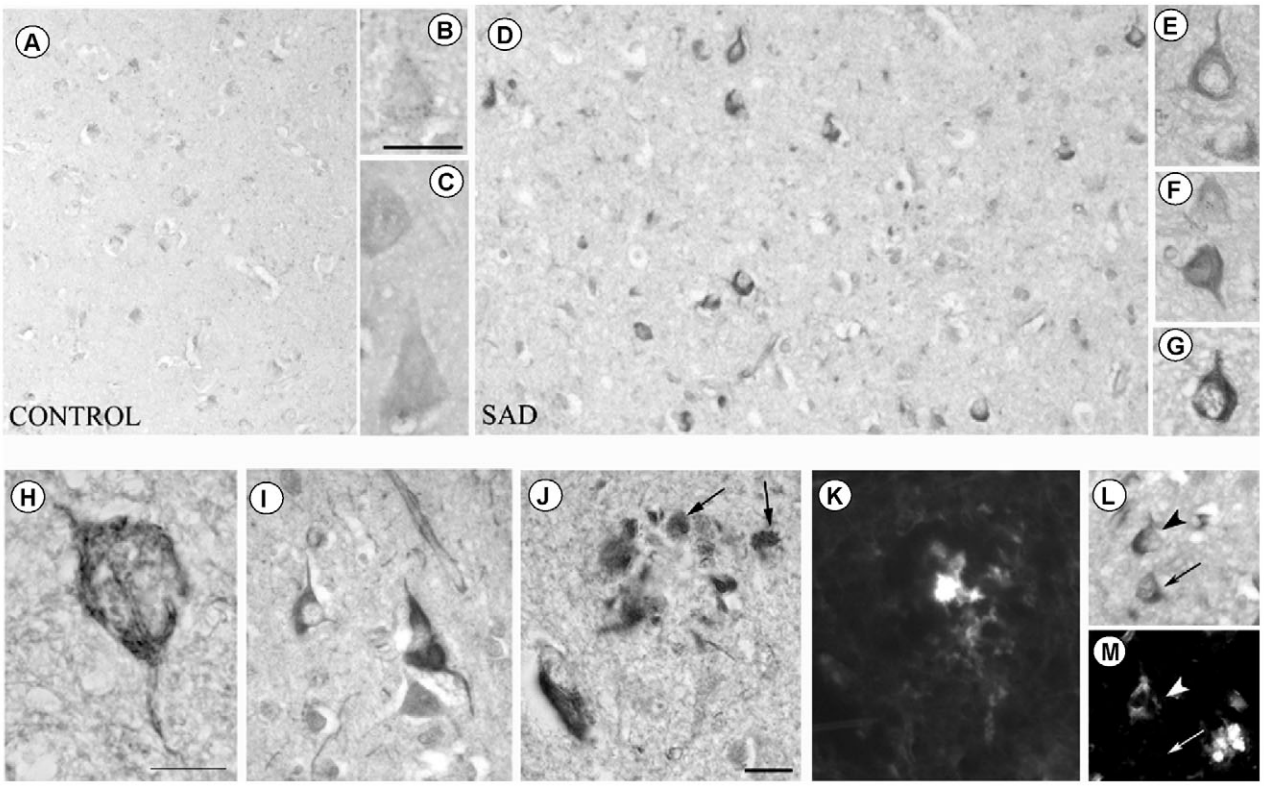

Fig. 10. Erasin immunocytochemistry in Alzheimer's disease and neuropathologically normal control brain. Paraffin sections (5 μm thickness) of prefrontal cortex immunolabeled with erasin 141 antibody show immunostaining patterns in neurons and within the neuropil from different cases of neuropathologically normal controls (A-C) and moderate to severe AD (SAD) (D-I). Immunoreactivity in control brains is minimal (A-C). Counterstaining with thioflavin-S reveals the location of neurofibrillary tangles in one erasin-positive neuron (arrowhead, L,M) but not in another (arrow, M versus L) and the location of β-amyloid peptide in a senile plaque (K) surrounded by erasin-positive dystrophic neurites (arrows in J). Bars, 5 μm.

that the membrane-targeting sequence of erasin resembles that of caveolin-1 and related molecules (reviewed by Ostermeyer et al., 2004). Interestingly, the membrane-targeting sequence of caveolin-1 when drawn on an α-helical wheel, suggests that it is composed of two very hydrophobic α-helices separated by a proline residue, which forms a kink, enabling the helices to interact with one another to form a coiled-coil structure (Ostermeyer et al., 2004). The coiled-coil structure is thought to insert directly into the membrane with the proline residue residing at the apex of the point of insertion. As shown in Fig. 5C we found that the membrane-targeting sequence of erasin when drawn on an α-wheel closely resembles that of caveolin-1, both in terms of the very hydrophobic nature of the sequence and the occurrence of a proline residue at the midpoint of the helical wheel. However, it is curious that the hydrophobic targeting sequence is only conserved in mammalian erasin homologs examined (see Fig. 1A), suggesting that this sequence might have evolved for a specific function in mammals. Alternatively, it is possible that the hydrophobic-targeting domain varies in location or sequence in other erasin homologs. According to the rest our model, we position the remainder of the erasin polypeptide, on the cytoplasmic and nucleoplasmic sides of the ER and NE, respectively, consistent with its ability to interact with p97/VCP.

Erasin is the first known mammalian UBX-domain-containing protein that has been localized to the ER or NE. The UBX domain is considered to be a general domain that is involved in binding p97/VCP and related proteins (Dreveny et al., 2004b; Schuberth et al., 2004; Hartmann-Petersen et al., 2004; Song et al., 2005). By co-immunoprecipitation and GST pull-down assays, we found that erasin binds p97/VCP, primarily through its UBX domain. It is interesting to note that the UBX domain of erasin contains a Phe-Pro sequence, in a position similar to that of the UBX domain of p47, which was found to be important for the binding p97/VCP (Dreveny et al., 2004a). Unlike erasin, p47 is believed to be a soluble protein present in both the cytosol and nucleus (Uchiyama et al., 2003).

In contrast to the mammalian UBX-containing proteins, recent evidence suggests that three of the seven UBX-containing proteins in yeast are localized to membranes (Ubx2, Ubx6, and Ubx7), possibly to the nuclear envelope and ER (Decottignies et al., 2004; Neuber et al., 2005; Schuberth and Buchberger, 2005). Two of the yeast proteins merit further discussion. The first is Ubx7, which shares highest homology (20% identity) with human erasin. However, we are not sure if Ubx7 and human erasin are homologs because we found that knockdown of erasin levels leads to almost complete inhibition of ERAD whereas a yeast strain deleted of the *UBX7* gene was reported to be unaltered in ERAD (Neuber et al., 2005). By contrast, yeast strains deleted on the *UBX2* gene displayed a property similar to that which we observed: inhibition of ERAD (Neuber et al., 2005; Schuberth and Buchberger, 2005).

Furthermore, Ubx2 protein expression, like erasin, is induced by ER stress (Neuber et al., 2005). Intriguingly, the yeast Ubx2 protein has a similar topology to that of erasin, with both its N- and C-termini exposed in the cytosol (Neuber et al., 2005; Schuberth and Buchberger, 2005). Although Ubx2 and erasin share similar functional properties and topology, the two proteins are quite different. Ubx2 is believed to contain two transmembrane domains whereas we propose that erasin has a single hydrophobic segment that is responsible for inserting the protein in membranes. In addition Ubx2 contains a UBA domain whereas erasin lacks such a domain.

The increase in erasin levels that we observed in cells exposed to ER stress agrees with our proposal that erasin functions in ERAD. It is well known that cells respond to ER stress by inducing a series of signal transduction cascades, collectively known as the unfolded protein response (UPR), as a means to correct and recover from the instigating insult(s) (reviewed by Schroder and Kaufman, 2005). Studies have revealed that there is intimate coordination of the UPR components with those involved in ERAD (Travers et al., 2000). We speculate that erasin levels increase in cells undergoing ER stress as a means to enhance clearance of misfolded proteins in the ER. In accordance with this notion we found that overexpression of *ERASIN* cDNA increased, albeit to a small extent, the degradation of CD3δ, a classical ERAD substrate. We offer two possible reasons why overexpression of *ERASIN* cDNA did not stimulate degradation of CD3δ more profoundly. First, under normal growth conditions erasin levels may already be optimal, and thus any further increase in its expression may not increase ERAD any more. Alternatively, and more likely, erasin probably functions in association with other ERAD factors, and these could be limiting in the cells in which we only overexpressed *ERASIN* cDNA. Obviously, under ER stress these additional factors, together with erasin, may be coordinately increased. The more crucial evidence demonstrating erasin functions in ERAD is that knockdown of erasin levels by RNAi almost completely abolished ERAD. Additionally we found that erasin exists in a complex in cells with two well-characterized ERAD components, the ubiquitin ligase gp78 and the putative ER-channel-forming protein Derlin-1, through which ERAD substrates are thought be retrotranslocated from the ER to the cytosol for degradation by the proteasome (Zhong et al., 2004; Lilley and Ploegh, 2004; Ye et al., 2004; Ye et al., 2005; Li et al., 2006). These results led us to speculate that erasin is probably an important component of ERAD.

The increase in anti-erasin staining in AD-afflicted brains is consistent with our cell culture experiments showing that erasin levels are increased during ER stress, suggesting that erasin activation is somehow linked to the UPR. This activation would agree with reports showing that proteins involved in UPR are increased in AD cases (Hamos et al., 1991; Hoozemans et al., 2005). Interestingly, we found erasin staining was principally increased in neurons undergoing neurofibrillary degeneration in AD suggesting that anti-erasin staining might be a useful tool for identifying AD pathology. Although we do not know the reason for the increase in erasin staining in AD brains, we speculate that it could reflect an attempt to stop misfolded proteins from building up in cells of the brain, which is a primary feature of AD (reviewed by Taylor et al., 2002). Alternatively, and less likely, the protein may be somehow involved in neurodegeneration. It is possible that the increased erasin staining of neurons lacking neurofibrillary tangles reflects the neurons that are at the beginning phase of neurodegeneration and which will eventually form tangles, suggesting that increased erasin expression may precede tangle formation in AD. It will be interesting to examine the time-course of erasin staining during neurodegeneration and its relationship to the disease process.

In conclusion, our results suggest that erasin is a novel NE- and ER-associated protein that is induced by ER stress, whose staining is increased in AD-afflicted brains, and which appears to function in ERAD. Further studies of erasin should lead to further insight into the role of this exciting new protein in cell function in normal and disease states.

Materials and Methods

Cloning and expression of untagged and tagged erasin proteins

We conducted a search of the human EST database to identify clones containing *ERASIN* cDNA fragments. By DNA sequencing, we found that one of them contained the complete *ERASIN* ORF. Mammalian expression of the *ERASIN* ORF was achieved using the CMV expression plasmid (Janicki and Monteiro, 1997). In addition to the untagged FL erasin expression construct, a Myc-tagged erasin construct was also prepared, fusing the Myc epitope in-frame at the C-terminus of the FL-*ERASIN* ORF. A series of CMV GFP-tagged erasin expression constructs were also constructed by fusing EGFP in-frame at either the C-terminus or N-terminus at different points along the *ERASIN* ORF. Immunoblots demonstrated that fusion proteins of the expected size were generated in all cases.

Northern blot analysis

The DNA insert of one of the erasin preys was radiolabeled with ^{32}P and used to probe a human multiple-tissue northern (MTN) blot and a human brain multiple-tissue northern blot II (Clontech) by DNA hybridization (Mah et al., 2000). The blots were then reprobed with a human β-actin cDNA control probe for RNA loading.

Polyclonal antibody production and characterization

The N-terminal portion of *ERASIN* ORF (residues 1 to 227aa) was expressed and purified as a GST-fusion protein. A synthetic peptide to a sequence in the C-terminus of erasin (residues 476-500) was synthesized and coupled to KLH carrier protein. The GST- and KLH-coupled erasin proteins were sent to Covance Research Products to generate in rabbits polyclonal antibodies 130 and 141, respectively. The specificity of antibody 141 was established by pre-incubating the antibody with different concentrations (0-1 mg/ml) of its cognate peptide for 2 hours, before immunoblotting.

In vitro transcription/translation and GST pull-down binding assay

[^{35}S]methionine-radiolabeled FL and partial erasin polypeptides were synthesized in rabbit reticulocyte lysates using a coupled in vitro transcription and translation system (Promega). The ^{35}S-labeled erasin proteins were incubated with 3 μg of purified GST or purified GST-p97(murine VCP), and binding of the proteins determined by GST pull-down assays, as described previously (Mah et al., 2000). For the p97/VCP pull-down assays the NP40 concentration in the wash buffer was increased to 0.75%.

Cell culture, DNA and siRNA transfection, immunofluorescence and electron microscopy

HeLa, HEK293 and U2OS cells were grown in DME supplemented with 10% FBS. NT2 cells were grown in modified DME containing 1.5 g/l sodium bicarbonate supplemented with 10% FBS. M059J cells were grown in a 1:1 mixture of DME and Ham's F12 medium supplemented with 10% FBS. Cells were transiently transfected with plasmid DNA using Lipofectamine™ 2000 (Invitrogen) or by calcium phosphate co-precipitation. siRNA (SMARTpool UBXD2) was transfected using DharmaFECT reagent 1 according to the protocol provided by the manufacturer (Dharmacon, Lafayette, CO). Immunofluorescence staining and fluorescence images of fixed and live cells were captured on a Leica DMIRB microscope with a PL Apo 100× lens (NA 1.4) using a Photometrics SenSys camera using IPLab software, essentially as described previously (Janicki and Monteiro, 1997). For EM, transfected HEK293 cells were fixed in 4% paraformaldehyde in 0.1 M HEPES buffer pH 7.4 for 30 minutes. They were then scraped, pelleted, and incubated in a solution of 2.3 M sucrose, 30% polyvinylpyrrolidone and frozen in liquid nitrogen. The cell pellets were then cut into thin (70 nm) sections on a

microtome and placed on formvar-coated nickel grids. They were stained with primary and 12-nm-gold-conjugated secondary antibodies using our standard protocol and then washed in PBS, fixed for 10 minutes in 2% glutaradehyde in PBS. The sections were finally washed in water, stained with 0.3% uranyl acetate in a 2% solution of methylcellulose and viewed under a Philips CM 120 electron microscope at 80 kV.

Protein preparation, SDS-PAGE, immunoprecipitation and immunoblotting

Cell and tissue protein lysates were prepared as described (Monteiro and Mical, 1996). Our standard protocol for protein separation and immunoblotting was followed (Mah et al., 2000). For immunoprecipitations assays, cells were lysed by homogenization in IP buffer (50 mM Tris-HCl, pH 7.5, 150 mM NaCl, 2 mM EDTA, 0.1% NP40, containing protease inhibitors) and after centrifugation at 3000 ***g*** for 10 minutes, the supernatant was recovered and used for the immunoprecipitations (Mah et al., 2000). For immunoprecipitation of Myc-tagged p97/VCP the concentration of NP40 was increased to 0.75%. In addition to our own rabbit polyclonal anti-erasin and monoclonal anti-gp78 antibodies we also used the following primary antibodies from commercial sources for immunoblotting immunoprecipitation: mouse monoclonal anti-canine GM130, anti-p97/VCP (Transduction Laboratories) anti-golgin 97 (Molecular Probes); anti-FLAG, and anti-HA (Sigma); rabbit polyclonal anti-calnexin-N, anti-calnexin-C, anti-calreticulin (StressGen), anti-CENP-B (gift from Dr Ann Pluta, JNCI, Washington, DC) and anti-Derlin-1 (MBL International); goat polyclonal anti-BiP and anti-actin (Santa Cruz Biotechnology).

Cell fractionation studies

HeLa cells were homogenized in 1 ml buffer B (0.25 M sucrose, 1 mM EDTA, 10 mM HEPES-NaOH, pH 7.4), then centrifuged at 3000 ***g*** for 10 minutes at 4°C, after which the supernatant was collected and layered on top of a 10 ml preformed 0-25% iodixanol gradient in buffer B. The layered gradients were then centrifuged at 200,000 ***g*** at 4°C for 2.5 hours in a Beckman SW 41Ti rotor. After centrifugation, fractions (0.65 ml) were collected from the bottom of the tube. An equal volume of each fraction was screened for proteins by immunoblotting.

Reticuloplasm, the luminal material of the endoplasmic reticulum (ER), was prepared as described (Macer and Koch, 1988). Subcellular fractionation of HeLa cell proteins in soluble and insoluble fractions by treatment with 1× PBS, 1 M NaCl, 0.1 M Na_2CO_3 (pH 11) or 1% Triton X-100 was described (Kokame et al., 2000). The proteinase K protection assay was also conducted according to the procedures described by these authors, except that microsome membranes were collected from HeLa cells and incubated with 0, 0.25, 1, 10 and 100 μg/ml proteinase K for 5 minutes; or 10 μg/ml, 100 μg/ml proteinase K for 1 hour.

Analysis of protein turnover

Protein degradation of the ERAD substrate CD3δ was measured in HEK293 cells over a 7.5 hour period after inhibition of protein synthesis by cycloheximide (Gardner et al., 2001; Sharma et al., 2004; Massey et al., 2005). For these analyses HEK293 cell cultures were cotransfected with a plasmid encoding HA-tagged CD3δ together with an *ERASIN* cDNA expression plasmid, or with an empty vector plasmid, or with *ERASIN* SMARTpool siRNA (Dharmacon). After transfection, the cultures were incubated with cycloheximide (final concentration 100 μM) and protein lysates were collected at different intervals thereafter, as indicted in the text. Equal amounts of protein from the different time points were then immunoblotted with anti-HA antibody (to detect Cd3δ), anti-erasin and anti-actin antibodies.

The turnover of GFP^u, a short-lived protein (Bence et al., 2001), was examined by classical pulse-chase analysis of [^{35}S]methionine-labeled proteins. For these analyses, cultures of a HEK293 cell line stably expressing the GFP^u protein (kindly provided by Dr Ron Kopito, Stanford University, Stanford, CA) were transfected either with an *ERASIN* cDNA expression plasmid, or with an empty vector plasmid, or with *ERASIN* SMARTpool siRNA. 20 hours after transfection, the cultures were labeled for 1 hour with [^{35}S]methionine and chased with nonradioactive medium for various periods as indicated, and the turnover of GFP was analyzed after immunoprecipitation of the protein, essentially as described previously (Mah et al., 2000).

Neuropathological examination of erasin immunoreactivity in human brain

Post-mortem, formalin-fixed tissue was obtained from the Harvard Brain Tissue Research Center at McLean Hospital (Belmont, MA). Tissue was examined using CERAD guidelines, Braak staging and the criteria proposed by Mirra et al. (Mirra et al., 1991; Mirra et al., 1993). Prefrontal cortices from seven cases diagnosed with moderate to severe AD (Braak stage VI), ranging in age from 60 to 77 years with a PMI of 20.10±3.79 hours, and from seven neuropathologically normal cases, ranging in age from 60 to 78 years with a PMI of 20.92±2.07 hours, were used for erasin immunocytochemical studies.

Immunocytochemistry was performed on 5 μm paraffin sections. Endogenous peroxidase activity was blocked using 0.3% hydrogen peroxide diluted in methanol and non-specific binding was blocked with 20% normal goat serum. Sections were incubated for 2 days at 4°C with anti-erasin antibody 141, diluted in TBS containing 0.9% NaCl, 2% BSA, 1% normal goat serum and 0.4% Triton X-100. Sections were incubated in biotinylated anti-rabbit for 30 minutes, in ABC reagent for 1 hour, visualized with DAB (Vector Labs, Burlingame, CA) and counterstained using 1% thioflavin-S diluted in 70% ethanol for 1 hour. Serial sections were processed using pre-immune serum to test specificity of antibody binding and thioflavin-S to determine that thioflavin binding was not blocked by antibody binding. Bielschowsky staining was performed on semi-adjacent sections. Microscopic analyses were performed using a Zeiss Axiovert 200M equipped with an AxioCam MRm digital camera (Carl Zeiss, Thornwood, NY).

This work was supported by a NIH grant GM066287 to MJM. We thank Dana Hartzman and Carol Cooke for kindly performing the Northern blot and EM, respectively. We thank Dr Caryoln Machamer for pointing out the similarity in membrane targeting of erasin with caveolin-1.

References

Bays, N. W., Wilhovsky, S. K., Goradia, A., Hodgkiss-Harlow, K. and Hampton, R. Y. (2001). HRD4/NPL4 is required for the proteasomal processing of ubiquitinated ER proteins. *Mol. Biol. Cell* **12**, 4114-4128.

Bence, N. F., Sampat, R. M. and Kopito, R. R. (2001). Impairment of the ubiquitin-proteasome system by protein aggregation. *Science* **292**, 1552-1555.

Braun, S., Matuschewski, K., Rape, M., Thoms, S. and Jentsch, S. (2002). Role of the ubiquitin-selective CDC48(UFD1/NPL4)chaperone (segregase) in ERAD of OLE1 and other substrates. *EMBO J.* **21**, 615-621.

Buchberger, A. (2002). From UBA to UBX: new words in the ubiquitin vocabulary. *Trends Cell Biol.* **12**, 216-221.

Buchberger, A., Howard, M. J., Proctor, M. and Bycroft, M. (2001). The UBX domain: a widespread ubiquitin-like module. *J. Mol. Biol.* **307**, 17-24.

Cao, K., Nakajima, R., Meyer, H. H. and Zheng, Y. (2003). The AAA-ATPase Cdc48/p97 regulates spindle disassembly at the end of mitosis. *Cell* **115**, 355-367.

Decottignies, A., Evain, A. and Ghislain, M. (2004). Binding of Cdc48p to a ubiquitin-related UBX domain from novel yeast proteins involved in intracellular proteolysis and sporulation. *Yeast* **21**, 127-139.

Dreveny, I., Kondo, H., Uchiyama, K., Shaw, A., Zhang, X. and Freemont, P. S. (2004a). Structural basis of the interaction between the AAA ATPase p97/VCP and its adaptor protein p47. *EMBO J.* **23**, 1030-1039.

Dreveny, I., Pye, V. E., Beuron, F., Briggs, L. C., Isaacson, R. L., Matthews, S. J., McKeown, C., Yuan, X., Zhang, X. and Freemont, P. S. (2004b). p97 and close encounters of every kind: a brief review. *Biochem. Soc. Trans.* **32**, 715-720.

Franke, W. W., Scheer, U., Krohne, G. and Jarasch, E. D. (1981). The nuclear envelope and the architecture of the nuclear periphery. *J. Cell Biol.* **91**, 39s-50s.

Gardner, R. G., Shearer, A. G. and Hampton, R. Y. (2001). In vivo action of the HRD ubiquitin ligase complex: mechanisms of endoplasmic reticulum quality control and sterol regulation. *Mol. Cell. Biol.* **21**, 4276-4291.

Hamos, J. E., Oblas, B., Pulaski-Salo, D., Welch, W. J., Bole, D. G. and Drachman, D. A. (1991). Expression of heat shock proteins in Alzheimer's disease. *Neurology* **41**, 345-350.

Hampton, R. Y. (2002). ER-associated degradation in protein quality control and cellular regulation. *Curr. Opin. Cell Biol.* **14**, 476-482.

Hartmann-Petersen, R., Wallace, M., Hofmann, K., Koch, G., Johnsen, A. H., Hendil, K. B. and Gordon, C. (2004). The ubx2 and ubx3 cofactors direct cdc48 activity to proteolytic and nonproteolytic ubiquitin-dependent processes. *Curr. Biol.* **14**, 824-828.

Hetzer, M., Meyer, H. H., Walther, T. C., Bilbao-Cortes, D., Warren, G. and Mattaj, I. W. (2001). Distinct AAA-ATPase p97 complexes function in discrete steps of nuclear assembly. *Nat. Cell Biol.* **3**, 1086-1091.

Hoozemans, J. J., Veerhuis, R., Van Haastert, E. S., Rozemuller, J. M., Baas, F., Eikelenboom, P. and Scheper, W. (2005). The unfolded protein response is activated in Alzheimer's disease. *Acta Neuropathol.* **110**, 165-172.

Janicki, S. and Monteiro, M. J. (1997). Increased apoptosis arising from increased expression of the Alzheimer's disease-associated presenilin-2 mutation (N141I). *J. Cell Biol.* **139**, 485-495.

Jarosch, E., Taxis, C., Volkwein, C., Bordallo, J., Finley, D., Wolf, D. H. and Sommer, T. (2002). Protein dislocation from the ER requires polyubiquitination and the AAA-ATPase Cdc48. *Nat. Cell Biol.* **4**, 134-139.

Klausner, R. D., Lippincott-Schwartz, J. and Bonifacino, J. S. (1990). The T cell antigen receptor: insights into organelle biology. *Annu. Rev. Cell Biol.* **6**, 403-431.

Kokame, K., Agarwala, K. L., Kato, H. and Miyata, T. (2000). Herp, a new ubiquitin-like membrane protein induced by endoplasmic reticulum stress. *J. Biol. Chem.* **275**, 32846-32853.

Kondo, H., Rabouille, C., Newman, R., Levine, T. P., Pappin, D., Freemont, P. and Warren, G. (1997). p47 is a cofactor for p97-mediated membrane fusion. *Nature* **388**, 75-78.

Li, G., Zhao, G., Zhou, X., Schindelin, H. and Lennarz, W. J. (2006). The AAA ATPase p97 links peptide N-glycanase to the endoplasmic reticulum-associated E3 ligase autocrine motility factor receptor. *Proc. Natl. Acad. Sci. USA* **103**, 8348-8353.

Lilley, B. N. and Ploegh, H. L. (2004). A membrane protein required for dislocation of misfolded proteins from the ER. *Nature* **429**, 834-840.

Macer, D. R. and Koch, G. L. (1988). Identification of a set of calcium-binding proteins

in reticuloplasm, the luminal content of the endoplasmic reticulum. *J. Cell Sci.* **91**, 61-70.

Mah, A. L., Perry, G., Smith, M. A. and Monteiro, M. J. (2000). Identification of ubiquilin, a novel presenilin interactor that increases presenilin protein accumulation. *J. Cell Biol.* **151**, 847-862.

Massey, L. K., Mah, A. L. and Monteiro, M. J. (2005). Ubiquilin regulates presenilin endoproteolysis and modulates gamma-secretase components, Pen-2 and nicastrin. *Biochem. J.* **391**, 513-525.

Meusser, B., Hirsch, C., Jarosch, E. and Sommer, T. (2005). ERAD: the long road to destruction. *Nat. Cell Biol.* **7**, 766-772.

Meyer, H. H., Shorter, J. G., Seemann, J., Pappin, D. and Warren, G. (2000). A complex of mammalian ufd1 and npl4 links the AAA-ATPase, p97, to ubiquitin and nuclear transport pathways. *EMBO J.* **19**, 2181-2192.

Mirra, S. S., Heyman, A., McKeel, D., Sumi, S. M., Crain, B. J., Brownlee, L. M., Vogel, F. S., Hughes, J. P., van Belle, G. and Berg, L. (1991). The consortium to establish a registry for Alzheimer's disease (CERAD). Part II. Standardization of the neuropathologic assessment of Alzheimer's disease. *Neurology* **41**, 479-486.

Mirra, S. S., Hart, M. N. and Terry, R. D. (1993). Making the diagnosis of Alzheimer's disease. A primer for practicing pathologists. *Arch. Pathol. Lab. Med.* **117**, 132-144.

Monteiro, M. J. and Mical, T. I. (1996). Resolution of kinase activities during the HeLa cell cycle: identification of kinases with cyclic activities. *Exp. Cell Res.* **223**, 443-451.

Nakamura, N., Rabouille, C., Watson, R., Nilsson, T., Hui, N., Slusarewicz, P., Kreis, T. E. and Warren, G. (1995). Characterization of a cis-Golgi matrix protein, GM130. *J. Cell Biol.* **131**, 1715-1726.

Neuber, O., Jarosch, E., Volkwein, C., Walter, J. and Sommer, T. (2005). Ubx2 links the Cdc48 complex to ER-associated protein degradation. *Nat. Cell Biol.* **7**, 993-998.

Oda, Y., Okada, T., Yoshida, H., Kaufman, R. J., Nagata, K. and Mori, K. (2006). Derlin-2 and Derlin-3 are regulated by the mammalian unfolded protein response and are required for ER-associated degradation. *J. Cell Biol.* **172**, 383-393.

Ostermeyer, A. G., Ramcharan, L. T., Zeng, Y., Lublin, D. M. and Brown, D. A. (2004). Role of the hydrophobic domain in targeting caveolin-1 to lipid droplets. *J. Cell Biol.* **164**, 69-78.

Rabinovich, E., Kerem, A., Frohlich, K. U., Diamant, N. and Bar-Nun, S. (2002). AAA-ATPase p97/Cdc48p, a cytosolic chaperone required for endoplasmic reticulum-associated protein degradation. *Mol. Cell. Biol.* **22**, 626-634.

Roy, L., Bergeron, J. J., Lavoie, C., Hendriks, R., Gushue, J., Fazel, A., Pelletier, A., Morre, D. J., Subramaniam, V. N., Hong, W. et al. (2000). Role of p97 and syntaxin 5 in the assembly of transitional endoplasmic reticulum. *Mol. Biol. Cell* **11**, 2529-2542.

Schroder, M. and Kaufman, R. J. (2005). The mammalian unfolded protein response. *Annu. Rev. Biochem.* **74**, 739-789.

Schuberth, C. and Buchberger, A. (2005). Membrane-bound Ubx2 recruits Cdc48 to ubiquitin ligases and their substrates to ensure efficient ER-associated protein degradation. *Nat. Cell Biol.* **7**, 999-1006.

Schuberth, C., Richly, H., Rumpf, S. and Buchberger, A. (2004). Shp1 and Ubx2 are adaptors of Cdc48 involved in ubiquitin-dependent protein degradation. *EMBO Rep.* **5**, 818-824.

Sharma, M., Pampinella, F., Nemes, C., Benharouga, M., So, J., Du, K., Bache, K. G., Papsin, B., Zerangue, N., Stenmark, H. et al. (2004). Misfolding diverts CFTR from recycling to degradation: quality control at early endosomes. *J. Cell Biol.* **164**, 923-933.

Song, E. J., Yim, S. H., Kim, E., Kim, N. S. and Lee, K. J. (2005). Human Fas-associated factor **1**, interacting with ubiquitinated proteins and valosin-containing protein, is involved in the ubiquitin-proteasome pathway. *Mol. Cell. Biol.* **25**, 2511-2524.

Taylor, J. P., Hardy, J. and Fischbeck, K. H. (2002). Toxic proteins in neurodegenerative disease. *Science* **296**, 1991-1995.

Travers, K. J., Patil, C. K., Wodicka, L., Lockhart, D. J., Weissman, J. S. and Walter, P. (2000). Functional and genomic analyses reveal an essential coordination between the unfolded protein response and ER-associated degradation. *Cell* **101**, 249-258.

Tsai, B., Ye, Y. and Rapoport, T. A. (2002). Retro-translocation of proteins from the endoplasmic reticulum into the cytosol. *Nat. Rev. Mol. Cell Biol.* **3**, 246-255.

Uchiyama, K., Jokitalo, E., Kano, F., Murata, M., Zhang, X., Canas, B., Newman, R., Rabouille, C., Pappin, D., Freemont, P. et al. (2002). VCIP135, a novel essential factor for p97/p47-mediated membrane fusion, is required for Golgi and ER assembly in vivo. *J. Cell Biol.* **159**, 855-866.

Uchiyama, K., Jokitalo, E., Lindman, M., Jackman, M., Kano, F., Murata, M., Zhang, X. and Kondo, H. (2003). The localization and phosphorylation of p47 are important for Golgi disassembly-assembly during the cell cycle. *J. Cell Biol.* **161**, 1067-1079.

Wada, I., Rindress, D., Cameron, P. H., Ou, W. J., Doherty, J. J., 2nd, Louvard, D., Bell, A. W., Dignard, D., Thomas, D. Y. and Bergeron, J. J. (1991). SSR alpha and associated calnexin are major calcium binding proteins of the endoplasmic reticulum membrane. *J. Biol. Chem.* **266**, 19599-19610.

Wang, Q., Song, C. and Li, C. C. (2004). Molecular perspectives on p97-VCP: progress in understanding its structure and diverse biological functions. *J. Struct. Biol.* **146**, 44-57.

Woodman, P. G. (2003). p97, a protein coping with multiple identities. *J. Cell Sci.* **116**, 4283-4290.

Ye, Y., Meyer, H. H. and Rapoport, T. A. (2001). The AAA ATPase Cdc48/p97 and its partners transport proteins from the ER into the cytosol. *Nature* **414**, 652-656.

Ye, Y., Shibata, Y., Yun, C., Ron, D. and Rapoport, T. A. (2004). A membrane protein complex mediates retro-translocation from the ER lumen into the cytosol. *Nature* **429**, 841-847.

Ye, Y., Shibata, Y., Kikkert, M., van Voorden, S., Wiertz, E. and Rapoport, T. A. (2005). Inaugural article: recruitment of the p97 ATPase and ubiquitin ligases to the site of retrotranslocation at the endoplasmic reticulum membrane. *Proc. Natl. Acad. Sci. USA* **102**, 14132-14138.

Yuan, X., Shaw, A., Zhang, X., Kondo, H., Lally, J., Freemont, P. S. and Matthews, S. (2001). Solution structure and interaction surface of the C-terminal domain from p47: a major p97-cofactor involved in SNARE disassembly. *J. Mol. Biol.* **311**, 255-263.

Zhong, X., Shen, Y., Ballar, P., Apostolou, A., Agami, R. and Fang, S. (2004). AAA ATPase p97/valosin-containing protein interacts with gp78, a ubiquitin ligase for endoplasmic reticulum-associated degradation. *J. Biol. Chem.* **279**, 45676-45684.